Observational Study

Medicine®

OPEN

Clinical application of MRI-respiratory gating technology in the evaluation of children with obstructive sleep apnea hypopnea syndrome

Guohui Zeng, MD[a], Yaoshu Teng, MD, PhD[a], Jin Zhu, MD[a,*], Darong Zhu, MD[b], Bin Yang, MD[b], Linpin Hu, MD[a], Manman Chen, MD[a], Xiao Fu, MD[a]

Abstract

The objective of the present study was to investigate the clinical application of magnetic resonance imaging (MRI)-respiratory gating technology for assessing illness severity in children with obstructive sleep apnea hypopnea syndrome (OSAHS).

MRI-respiratory gating technology was used to scan the nasopharyngeal cavities of 51 children diagnosed with OSAHS during 6 respiratory phases. Correlations between the ratio of the area of the adenoid to the area of the nasopalatine pharyngeal cavity (Sa/Snp), with the main indexes of polysomnography (PSG), were analyzed. Receiver operator characteristic (ROC) curve and Kappa analysis were used to determine the diagnostic accuracy of Sa/Snp in pediatric OSAHS.

The Sa/Snp was positively correlated with the apnea hypopnea index (AHI) ($P < .001$) and negatively correlated with the lowest oxygen saturation of blood during sleep ($LaSO_2$) ($P < .001$). ROC analysis in the 6 respiratory phases showed that the area under the curve (AUC) of the Sa/Snp in the end-expiratory phase was the largest (0.992, $P < .001$), providing a threshold of 69.5% for the diagnosis of severe versus slight-moderate OSAHS in children. Consistency analysis with the AHI showed a diagnosis accordance rate of 96.0% in severe pediatric OSAHS and 96.2% in slight-moderate pediatric OSAHS (Kappa = 0.922, $P < .001$).

Stenosis of the nasopalatine pharyngeal cavity in children with adenoidal hypertrophy was greatest at the end-expiration phase during sleep. The end-expiratory Sa/Snp obtained by a combination of MRI and respiratory gating technology has potential as an important imaging index for diagnosing and evaluating severity in pediatric OSAHS.

Abbreviations: A/N = adenoid-nasal pharyngeal cavity ratio, AHI = apnea hypopnea index, CT = computed tomography, FOV = field of view, $LaSO_2$ = lowest oxygen saturation of blood, MRI = magnetic resonance imaging, OSAHS = obstructive sleep apnea hypopnea syndrome, PSG = polysomnography, ROS = receiver operator characteristic, TE = echo time, TR = repetition time.

Keywords: adenoids, magnetic resonance imaging, obstructive, respiratory-gated imaging techniques, sleep apnea

1. Introduction

Obstructive sleep apnea hypopnea syndrome (OSAHS) is a common sleep-related respiratory disorder. Its prevalence is approximately 2% in children, but primary snoring is reported to be more common, ranging from 3% to 12%.[1] OSAHS is characterized by repetitive obstruction in the upper airway during sleep, which may be partial or complete, and causes hypopnea or apnea, respectively.[1–3] In most cases of pediatric OSAHS, upper airway obstruction occurs from the nasopharynx to the oropharynx, caused by upper airway stenosis resulting from adenoid and tonsil hypertrophy with soft tissue collapse around the airway. The most common pathogenesis of pediatric OSAHS is adenoidal hypertrophy.

In OSAHS, breathing is labored during sleep due to obstruction of the upper airway. As a result, nocturnal oxygen saturation is decreased and sleep is fragmented leading to a decrease in memory, cognitive competence, attention, and control, as well as a series of pathological changes, including maxillofacial malformations and growth disorders.[4] If the condition is not recognized and treated early, OSAHS can seriously affect the growth and development of a child. Therefore, interest in OSAHS has increased in healthcare settings.

Polysomnography (PSG) is the current gold standard for diagnosing pediatric OSAHS as it can accurately determine the adverse effects of OSAHS on multiple physiological functions.[5] However, PSG is limited as it cannot accurately localize the stenotic site in an OSAHS patient's upper airway, and in young patients, PSG is relatively complicated as continual monitoring is required. Furthermore, other factors, such as loose electrodes and poor skin contact can influence test results.

Recently, researchers have focused on imaging studies that can locate the precise site and severity of the obstruction in OSAHS.[6,7] During sleep, upper airway morphology can change with inspiration and expiration; hence, dynamic imaging to objectively assess the level and extent of the obstruction in the upper airway is important. As a noninvasive and nonirradiative dynamic imaging method with a high resolution for soft tissues,

Editor: Giuseppe Insalaco.

Funding: This work was supported by grants from Science and Technology Plan Program of Zhejiang Province (no. 2012C33036) and Science and Technology Development Project of Hangzhou (no. 20160533B07).

The authors have no conflicts of interest to disclose.

[a] Department of Otorhinolaryngology Head and Neck Surgery, [b] Department of Radiology, Hangzhou First People's Hospital, Zhejiang Chinese Medical University, Hangzhou, China.

[*] Correspondence: Jin Zhu, Department of Otorhinolaryngology Head and Neck Surgery, Hangzhou First People's Hospital, Zhejiang Chinese Medical University, Hangzhou 310006, China (e-mail: zhujin2698@163.com).

Medicine (2018) 97:4(e9680)

Received: 19 July 2017 / Received in final form: 11 December 2017 / Accepted: 28 December 2017

http://dx.doi.org/10.1097/MD.0000000000009680

magnetic resonance imaging (MRI) is increasingly being applied for the diagnosis of OSAHS.

The objective of the present study was to investigate the clinical application of MRI-respiratory gating technology for assessing illness severity in children with OSAHS. A combination of MRI and respiratory gating technology was used to observe the dynamic changes of the upper airway nasopalatine pharyngeal cavity at different respiratory phases. The ratio of the area of the adenoid to the area of the nasopalatine pharyngeal cavity on median sagittal images was compared with the main indices of PSG.

2. Materials and methods

2.1. Clinical data

Children with OSAHS diagnosed in the Department of Otorhinolaryngology, Hangzhou First People's Hospital, Zhejiang Chinese Medical University between December 2012 and May 2015 were eligible for this study. Inclusion criteria were: diagnosis of OSAHS by PSG (Embletta X100, Embla, Broomfield, CO); and apnea hypopnea index (AHI) > 5. Exclusion criteria were upper airway obstruction due to grade II or higher tonsil hypertrophy or other diseases; or obesity, defined according to the BMI Reference Norm for Screening Overweight and Obesity in Chinese Children and Adolescents. The study was approved by the ethical committee of the Hangzhou First People's Hospital, and written informed consent was obtained from the families of all the children.

2.2. MRI scanning and image measurement

2.2.1. Preparations before MRI scanning. An MRI scanner (Magetom Verio3.0-Tesla, Siemens, Germany) was used to scan the upper airways of children with OSAHS. All children were sedated with 10% chloral hydrate (0.5 mg/kg body weight, total volume <25 mL) or an intramuscular injection of phenergan (0.5–1 mg/kg body weight). Children were placed in a supine position on the examination table. A neck coil was used for MRI scanning.

2.2.2. Respiratory gated dynamic upper airway imaging. Respiratory gated dynamic upper airway images were obtained using a TrueFISP sequence with the following parameters: repetition time (TR) = 4.6 milliseconds, echo time (TE) = 2.3 milliseconds, field of view (FOV) = 200 mm × 15 mm, matrix = 256 × 192, half-Fourier acquisition with the acquisition time = 300 milliseconds/slice, and slice thickness = 3.0 mm. For cross-sectional scanning, sagittal images of the upper airway were used for positioning, and the area from the cranial base to the laryngopharynx level was scanned. For sagittal scanning, cross-sectional images were used for positioning, and the whole adenoid and nasopalatine pharyngeal cavity was scanned (Fig. 1). The Siemens Verio gating system was used for respiratory gating, whereby a respiratory gating sensor was placed on the child's abdomen and tightened by a belly band. Inspiration/expiration phase was selected in the parameter view, and thresholds (10%, 50%, and 90% of the inspiration/expiration phase) were selected (Fig. 2). Respiratory triggered simultaneous cross-sectional and sagittal scanning was performed in 6 respiratory phases, including at 10% (initial), 50% (mid), and 90% (end) of the inspiration and the expiration phase.

2.3. MRI analysis

The adenoid (a) and nasopalatine pharyngeal cavity (np) were drawn on median sagittal images of the nasopalatine pharyngeal

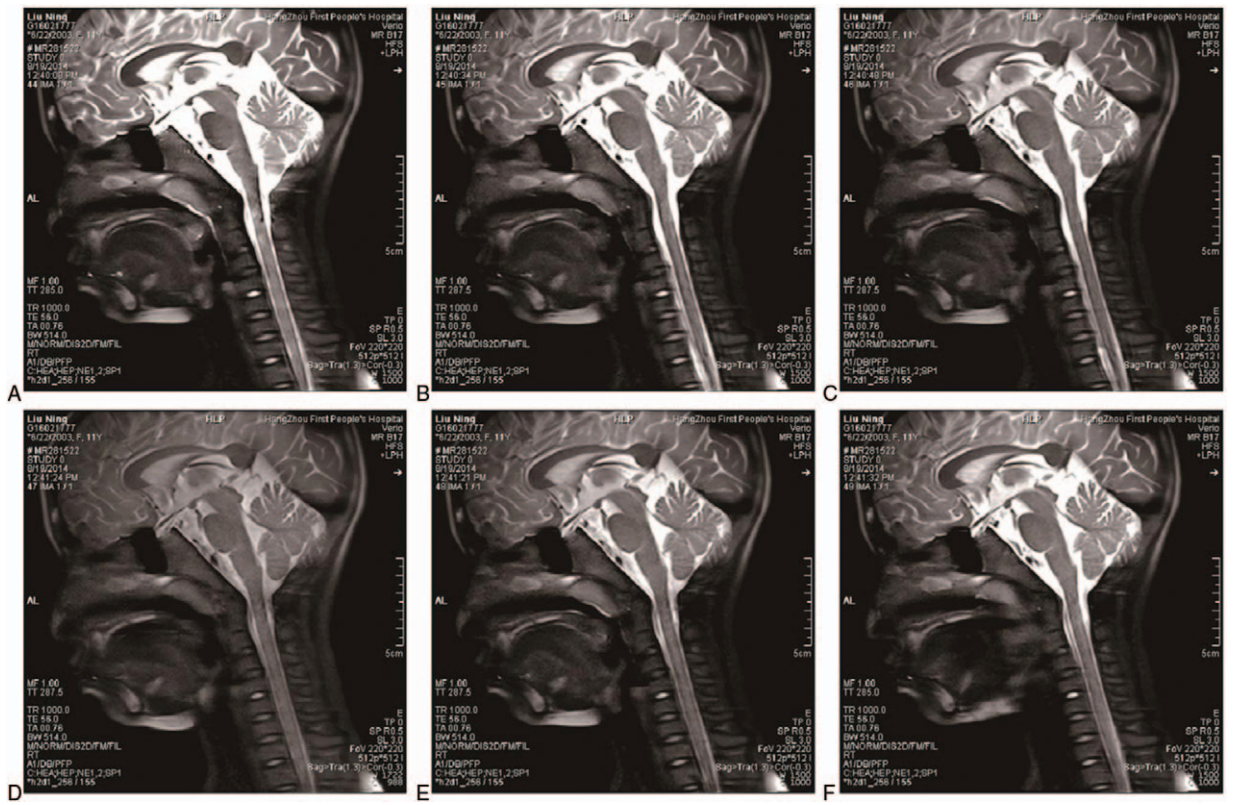

Figure 1. Median sagittal MRI of the upper airway at the 6 respiratory phases. (A–C) Sagittal MR images of the upper airway at 10%, 50%, and 90% of the inspiration phases. (D–F) Sagittal MRI of the upper airway at 10%, 50%, and 90% of the expiration phases.

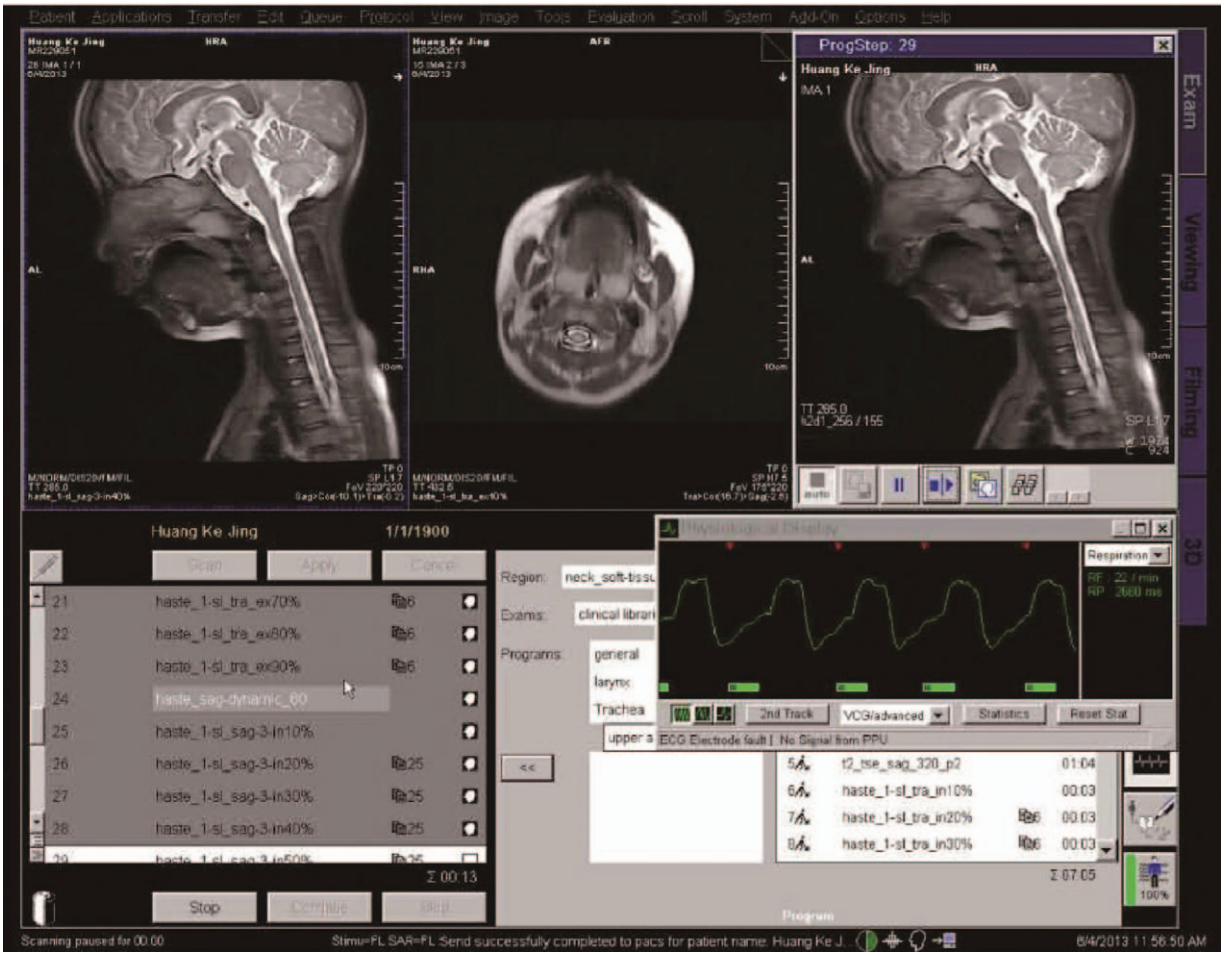

Figure 2. Panel for setting the parameters of the MRI-respiratory gating technology.

cavity during the 6 respiratory phases. The areas of the adenoid (Sa) and nasopalatine pharyngeal cavity (Snp) were measured (Fig. 3), and the Sa/Snp at each respiratory phase was calculated.

2.4. Statistical analysis

Statistical analyses were performed with SPSS 19.0 software (IBM, IL). Data are expressed as mean ± SD. Normality of data was assessed using the Kolmogorov–Smirnov test. Between-group comparisons were analyzed by repeated measures analysis of variance. Correlation was performed with Pearson correlation analysis, and receiver operator characteristic (ROC) curve analysis was applied to estimate sensitivity and specificity. Consistency analysis was performed using the Kappa test. $P < .05$ was considered statistically significant.

3. Results

This study included 51 children with OSAHS. Mean age of the children was 5.8 ± 2.0 years (3–13 years), mean AHI value was 20.0 ± 8.0, and mean lowest arterial oxygen saturation ($LaSO_2$) was 77.3 ± 10.1% (Table 1).

3.1. Sa/Snp at different respiratory phases in the median sagittal plane

To evaluate the degree of nasopalatine pharyngeal cavity obstruction in children with OSAHS and adenoidal hypertrophy throughout different respiratory phases, we calculated the Sa/Snp

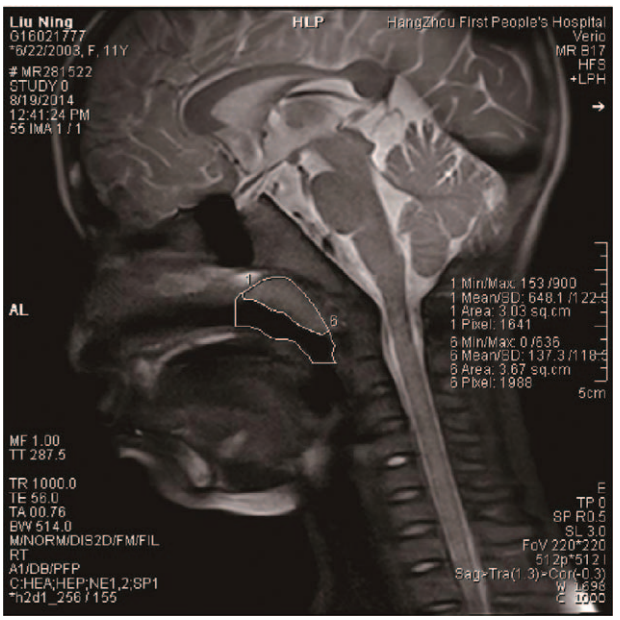

Figure 3. Areas of the adenoids and nasopalatine pharyngeal cavity in the median sagittal MRI of the upper airway (the entire marked area highlighted the median sagittal area of the nasopalatine pharyngeal cavity, while the grey separate area within the marked area indicated the median sagittal area of the adenoid).

Table 1

Clinical features of 51 children with OSAHS.

	Mean ± SD
Age, y	5.8 ± 2.0
BMI	16.0 ± 2.5
AHI	20.0 ± 8.0
$LaSO_2$ (%)	77.3 ± 10.1

AHI = apnea hypopnea index, BMI = body mass index, SD = standard deviation.

Table 2

The Sa/Snp of pediatric OSAHS at different respiratory phases.

	Sa/Snp (%, $\bar{x} \pm S$)					
	Initial inspiration	Mid-inspiration	End-inspiration	Initial expiration	Mid-expiration	End-expiration
Mean	64.94	62.92	59.96	61.69	64.82	68.96
SD	13.11	12.79	10.65	12.98	12.96	13.24
F			39.30*			
P			<.001**			

SD = standard deviation.
* Repeated measures analysis of variance.
** *P*-value was corrected by G-G coefficient.

in the 6 respiratory phases determined by MRI of the upper airway. Sa/Snp at initial inspiration, mid-inspiration, end-inspiration, initial expiration, mid-expiration, and end-expiration was 64.94 ± 13.11%, 62.92 ± 12.79%, 59.96 ± 10.65%, 61.69 ± 12.98%, 64.82 ± 12.96%, and 68.96 ± 13.24%, respectively, with a statistical significance (F = 39.3, $P < .001$; Table 2). Pairwise comparisons showed statistical significance between each phase of inspiration and expiration except mid-inspiration and mid-expiration, and end-inspiration and initial expiration. Furthermore, the Sa/Snp was significantly higher at end-expiration compared to the other 5 respiratory phases ($P < .001$; Table 3).

3.2. Correlation of Sa/Snp with the main indices of PSG throughout different respiratory phases

To evaluate the correlation of the Sa/Snp obtained by MRI of the upper airway with the main indices of PSG in the 6 respiratory phases, the Sa/Snp was correlated with the AHI and $LaSO_2$ during sleep. The Sa/Snp was positively correlated with the AHI ($P < .001$). The largest correlation coefficient was found between the Sa/Snp and the AHI in the end-expiration phase (0.933). The Sa/Snp was negatively correlated with the $LaSO_2$ ($P < .001$); the largest correlation coefficient was found between the Sa/Snp and the $LaSO_2$ in the end-expiration phase (−0.858; Table 4).

3.3. Sa/Snp threshold for classifying severity of illness in pediatric OSAHS patients

To generate a Sa/Snp threshold for classifying severity of illness in pediatric OSAHS patients, AHI was used as the gold standard for severity judgment (patients with AHI > 20 were considered severe, and patients with AHI ≤ 20 were considered slight-moderate). ROC analysis in the 6 respiratory phases showed that the AUC of the Sa/Snp in the end-expiratory phase was the largest (0.992, $P < .001$), providing a threshold of 69.5% for the diagnosis of severe versus slight-moderate OSAHS in children (Fig. 4).

Table 3

Pairwise comparison of the Sa/Snp of pediatric OSAHS at different respiratory phases.

Comparison of different respiratory phases	Difference in means	*P**
Initial inspiration vs mid-inspiration	2.02	.07
Initial inspiration vs end-inspiration	4.98	<.001
Initial inspiration vs initial expiration	3.25	.007
Initial inspiration vs mid-expiration	0.12	1.00
Initial inspiration vs end-expiration	−4.02	<.001
Mid-inspiration vs end-inspiration	3.00	.048
Mid-inspiration vs initial expiration	1.27	.397
Mid-inspiration vs mid-expiration	−1.86	.191
Mid-inspiration vs end-expiration	−6.00	<.001
End-inspiration vs initial expiration	−1.73	1.00
End-inspiration vs mid-expiration	−4.86	<.001
End-inspiration vs end-expiration	−9.00	<.001
Initial expiration vs mid-expiration	−3.13	.032
Initial expiration vs end-expiration	−7.27	<.001
Mid-inspiration vs end-expiration	−4.132.45	<.001

* Bonferroni corrected *P*-value.

3.4. Diagnosis accordance rate of Sa/Snp at end-expiration and AHI

Based on an end-expiratory Sa/Snp of 69.50%, pediatric OSAHS patients were divided into severe and slight-moderate groups. Consistency analysis with outcomes of AHI classification showed a diagnosis accordance rate of 96.0% in severe pediatric OSAHS and 96.2% in slight-moderate pediatric OSAHS (Kappa = 0.922, $P < .001$; Table 5).

4. Discussion

A relative change in the volumes of the adenoid and the nasopalatine pharyngeal cavities during respiration is the main reason for nasopalatine pharyngeal cavity obstruction. Therefore, in this study, we explored the utility of the Sa/Snp obtained by median sagittal MRI as an index of the degree of obstruction of the nasopalatine pharyngeal cavity in pediatric OSAHS. Findings showed that the Sa/Snp was gradually decreased from initial inspiration to end-inspiration, suggesting that the volume of the upper airway was increased, and obstruction of the nasopalatine pharyngeal cavity was gradually alleviated. During expiration, the Sa/Snp was gradually increased, reaching a maximum at end-expiration, indicating that the degree of stenosis at end-expiration was the most severe. Inspiration is an active process, and the tension of the upper airway dilator muscles is increased by an enlarged airway volume. Conversely, expiration is a passive process, and during sleep, there is a reduction in muscle tone in the thorax, abdomen, and pharynx. We speculate

Table 4

Correlation coefficient (r) of the Sa/Snp at each respiratory phase with the AHI and $LaSO_2$.

PSG index	Sa/Snp					
	Initial inspiration	Mid-inspiration	End-inspiration	Initial expiration	Mid-expiration	End-expiration
AHI	0.897	0.869	0.763	0.789	0.901	0.933
$LaSO_2$	−0.856	−0.825	−0.655	−0.766	−0.812	−0.858

AHI = apnea hypopnea index, PSG = polysomnography.
* All the correlation coefficient had $P < .001$.

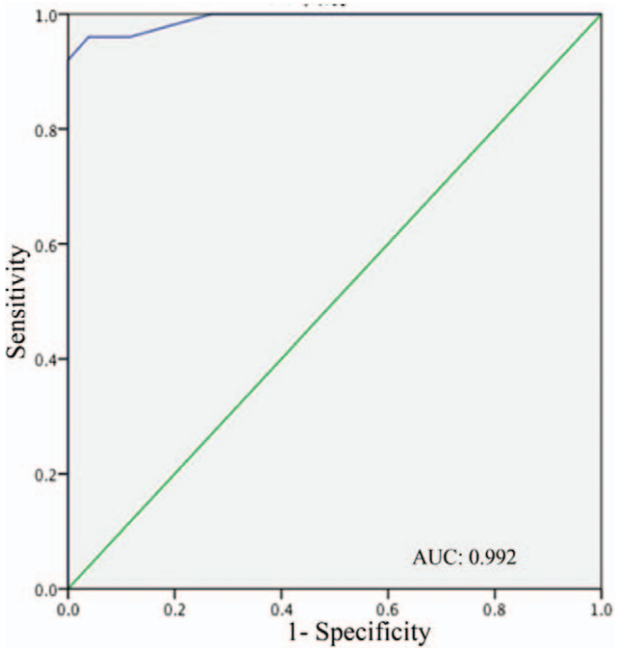

Figure 4. The ROC curve of the Sa/Snp at end-expiration phase.

that airflow impacts the soft palate during expiration, elevating it toward the nasopalatine pharyngeal cavity, resulting in stenosis.

PSG is the current gold standard for diagnosing and evaluating the severity of OSAHS. We found a positive correlation between the Sa/Snp and the PSG main index (AHI), and a negative correlation between the Sa/Snp and the $LaSO_2$ during all 6 respiratory phases. This suggests that the Sa/Snp obtained using MRI-respiratory gating technology has potential as an important imaging index for the diagnosis of pediatric OSAHS. Furthermore, our study found that the end-expiratory Sa/Snp had the highest correlation with the AHI and $LaSO_2$, and the largest AUC in ROC analysis, providing a threshold of 69.5% for the diagnosis of severe versus slight-moderate OSAHS in children. Consistency analysis with outcomes of AHI classification showed a diagnosis accordance rate of 96.0% in severe pediatric OSAHS and 96.2% in slight-moderate pediatric OSAHS. These rates were significantly higher than those reported in a previous consistency analysis of the adenoid–nasal pharyngeal cavity ratio (A/N) measured on computed tomography (CT) with PSG.[8] These data suggest that the Sa/Snp has high accuracy for the evaluation of pediatric OSAHS severity. Clinically, pediatric OSAHS may be diagnosed as severe if the Sa/Snp is ≥70%, or slight-moderate if the Sa/Snp is <70%.

Evidence suggests that anatomic stenosis of the upper airway and local soft tissue collapse are the main causes of OSAHS, but the characteristics of OSAHS in children and adults are different. The onset of pediatric OSAHS is mainly due to pathologic soft tissue hyperplasia and hypertrophy in the upper airway, including abnormal proliferation of the lymphoid tissues (adenoid and tonsil). Of these, adenoid hyperplasia is the most common, occurring frequently in children 3 to 6 years of age.[9,10] The adenoids lie in the nasopalatine pharyngeal cavity wall, forming part of the pharyngeal lymphoid ring; the adenoids form the first line of defense against pathogens in the respiratory tract. Inflammation of the adenoids causes pathological hyperplasia and nasopalatine pharyngeal cavity obstruction. Generally, surgical intervention in pediatric OSAHS is reserved for severe disease and when conservative treatments fail.[11] Therefore, accurately judging the degree of adenoid hyperplasia and its impact on the nasopalatine pharyngeal cavity is essential for clinical decision making.

The use of electronic nasopharyngeal endoscopy for OSAHS diagnosis is difficult in small children due to poor patient cooperation. Thus, noninvasive medical imaging technology is often applied to diagnose the obstructive site in pediatric OSAHS patients. Fujioka et al[8] proposed that the degree of adenoidal hypertrophy obstruction could be judged by measuring the A/N via a lateral cephalometric radiograph. However, their study was conducted at a single point in time in "awake" children. As respiration is a dynamic process, it is difficult to comprehensively and accurately evaluate the actual degree of stenosis of the nasopalatine pharyngeal cavity as a linear ratio in an instantaneous plane in children in an "awake" state. Children with OSAHS in the "awake" state rarely have symptoms of upper airway obstruction, and anatomical structural changes only become evident when a child is asleep. McGinley et al[12] proposed that the difference in respiratory tract morphology between the sleep and "awake" states might be related to the lack of a local neuromuscular compensatory function and an increase in soft tissue compliance during the sleep state.

The use of CT for the diagnosis of pediatric OSAHS is not appropriate as CT has poor resolution in soft tissue, which is easily damaged by exposure to radioactivity. In contrast, MRI is advantageous in OSAHS as it has high resolution in soft tissues, no radiation, and slice selection.[13,14] With the development and application of fast scanning sequences, MRI has become an important technique in OSAHS research.[15,16] In fact, a combination of MRI and respiratory gating technology can provide dynamic airway images at different respiratory phases and measure the parameters of structures in the upper airways.

Accordingly, to explore changes in the nasopalatine pharyngeal cavity in pediatric OSAHS, we performed upper airway MRI during sleep. As dynamic changes in soft palate morphology during respiration represent an important pathogenic factor in OSAHS,[17] we focused our studies on the nasopalatine pharyngeal cavity above the plane of the soft palate. In order to exclude multiple confounding factors, our study population included pediatric OSAHS patients with adenoidal hypertrophy

Table 5

Diagnosis accordance rate of Sa/Snp at end-expiration phase and AHI.

AHI classification	n	End-expiratory Sa/Snp classification		Kappa	*P*
		Slight-moderate (Sa/Snp ≤ 69.50%), (n, %)	Severe (Sa/Snp > 69.50%), (n, %)		
Slight-moderate (AHI ≤ 20)	26	25 (96.2%)	1 (3.8%)	0.922	<.001
Severe (AHI > 20)	25	1 (4.0%)	24 (96.0%)		

AHI = apnea hypopnea index.

alone. Furthermore, we focused on the dynamic changes on the median sagittal image of the nasopalatine pharyngeal cavity during respiration, as the median sagittal image can be accurately located. However, our findings must be interpreted with caution as they are preliminary. It is unknown whether these data apply to pediatric OSAHS caused by upper airway multisite stenosis or if they indicate the need for surgical intervention.

Obesity is a common cause of adult and pediatric OSAHS. However, obesity could result in false-negative diagnosis of pediatric OSAHS without adenoidal hypertrophy by our MRI scanning technique. Accordingly, obese children were not included in our study. In addition, there are some other limitations of MRI in the diagnosis of OSAHS. Pediatric OSAHS patients must be sedated before MRI scanning, which carries a risk of respiratory depression. Furthermore, MRI-respiratory gating technology requires highly trained professional imaging staff.

5. Conclusions

Stenosis of the nasopalatine pharyngeal cavity in children with adenoidal hypertrophy was greatest at the end-expiration phase during sleep. The end-expiratory Sa/Snp obtained by a combination of MRI and respiratory gating technology has potential as an important imaging index for diagnosing and evaluating severity in pediatric OSAHS.

References

[1] Xu Z, Cheuk DK, Lee SL. Clinical evaluation in predicting childhood obstructive sleep apnea. Chest 2006;130:1765–71.
[2] Malhotra A, White DP. Obstructive sleep apnoea. Lancet 2002;360:237–45.
[3] Sanchez-Armengol A, Fuentes-Pradera MA, Capote-Gil F, et al. Sleep-related breathing disorders in adolescents aged 12 to 16 years: clinical and polygraphic findings. Chest 2001;119:1393–400.
[4] Guilleminault C, Lee JH, Chan A. Pediatric obstructive sleep apnea syndrome. Arch Pediatr Adolesc Med 2005;159:775–85.
[5] Heo JY, Kim JS. Correlation between severity of sleep apnea and upper airway morphology: cephalometry and MD-CT study during awake and sleep states. Acta Otolaryngol 2011;131:84–90.
[6] Persak SC, Sin S, McDonough JM, et al. Noninvasive estimation of pharyngeal airway resistance and compliance in children based on volume-gated dynamic MRI and computational fluid dynamics. J Appl Physiol (1985) 2011;111:1819–27.
[7] Tang XL, Yi HL, Luo HP, et al. The application of CT to localize the upper airway obstruction plane in patients with OSAHS. Otolaryngol Head Neck Surg 2012;147:1148–53.
[8] Fujioka M, Young LW, Girdany BR. Radiographic evaluation of adenoidal size in children: adenoidal-nasopharyngeal ratio. AJR Am J Roentgenol 1979;133:401–4.
[9] Schwab RJ, Kim C, Bagchi S, et al. Understanding the anatomic basis for obstructive sleep apnea syndrome in adolescents. Am J Respir Crit Care Med 2015;191:1295–309.
[10] Slaats MA, Van Hoorenbeeck K, Van Eyck A, et al. Upper airway imaging in pediatric obstructive sleep apnea syndrome. Sleep Med Rev 2015;21:59–71.
[11] Friedman M, Wilson M, Lin HC, et al. Updated systematic review of tonsillectomy and adenoidectomy for treatment of pediatric obstructive sleep apnea/hypopnea syndrome. Otolaryngol Head Neck Surg 2009;140:800–8.
[12] McGinley BM, Schwartz AR, Schneider H, et al. Upper airway neuromuscular compensation during sleep is defective in obstructive sleep apnea. J Appl Physiol (1985) 2008;105:197–205.
[13] Suratt PM, Dee P, Atkinson RL, et al. Fluoroscopic and computed tomographic features of the pharyngeal airway in obstructive sleep apnea. Am Rev Respir Dis 1983;127:487–92.
[14] Xiao Y, Chen X, Shi H, et al. Evaluation of airway obstruction at soft palate level in male patients with obstructive sleep apnea/hypopnea syndrome: dynamic 3-dimensional CT imaging of upper airway. J Huazhong Univ Sci Technolog Med Sci 2011;31:413–8.
[15] Chen YJ, Shih TT, Chang YC, et al. Acoustic-integrated dynamic MR imaging for a patient with obstructive sleep apnea. Magn Reson Imaging 2015;33:1350–2.
[16] Morrell MJ, Arabi Y, Zahn B, et al. Progressive retropalatal narrowing preceding obstructive apnea. Am J Respir Crit Care Med 1998;158: 1974–81.
[17] Subramaniam DR, Mylavarapu G, Mcconnell K, et al. Upper airway elasticity estimation in pediatric Down syndrome sleep apnea patients using collapsible tube theory. Ann Biomed Eng 2016;44:1538–52.